

Mechanistic Studies of Photoinduced Spin Crossover and Electron Transfer in Inorganic Complexes

Published as part of the *Accounts of Chemical Research* special issue "Ultrafast Excited-State Processes in Inorganic Systems".

Wenkai Zhang[†] and Kelly J. Gaffney^{*,‡}

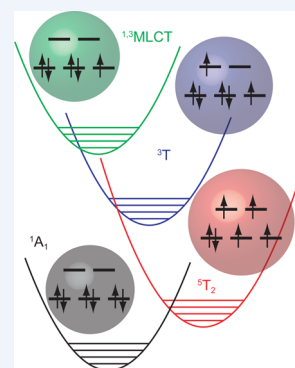
[†]Department of Chemistry, University of Pennsylvania, Philadelphia, Pennsylvania 19104, United States

[‡]Stanford Synchrotron Radiation Laboratory and PULSE Institute, SLAC National Accelerator Laboratory, Stanford University, Menlo Park, California 94025, United States

CONSPECTUS: Electronic excited-state phenomena provide a compelling intersection of fundamental and applied research interests in the chemical sciences. This holds true for coordination chemistry, where harnessing the strong optical absorption and photocatalytic activity of compounds depends on our ability to control fundamental physical and chemical phenomena associated with the nonadiabatic dynamics of electronic excited states. The central events of excited-state chemistry can critically influence the dynamics of electronic excited states, including internal conversion (transitions between distinct electronic states) and intersystem crossing (transitions between electronic states with different spin multiplicities), events governed by nonadiabatic interactions between electronic states in close proximity to conical intersections, as well as solvation and electron transfer. The diversity of electronic and nuclear dynamics also makes the robust interpretation of experimental measurements challenging. Developments in theory, simulation, and experiment can all help address the interpretation and understanding of chemical dynamics in organometallic and coordination chemistry. Synthesis presents the opportunity to chemically engineer the strength and symmetry of the metal–ligand interactions.

This chemical control can be exploited to understand the influence of electronic ground state properties on electronic excited-state dynamics. New time-resolved experimental methods and the insightful exploitation of established methods have an important role in understanding, and ideally controlling, the photophysics and photochemistry of transition metal complexes. Techniques that can disentangle the coupled motion of electrons and nuclear dynamics warrant emphasis.

We present a review of electron localization dynamics in charge transfer excited states and the dynamics of photoinitiated spin crossover dynamics. Both electron localization and spin crossover have been investigated by numerous research groups with femtosecond resolution spectroscopy, but challenges in experimental interpretation have left significant uncertainty about the molecular properties that control these phenomena. Our Account will emphasize how tailoring the experimental probe, femtosecond resolution vibrational anisotropy for electron localization, and femtosecond resolution hard X-ray fluorescence for spin crossover can make a significant impact on the interpretability of experimental measurements. The emphasis on thorough and robust interpretation has also led to an emphasis on simpler molecular systems. This enables iteration between experiment and theory, a requirement for the development of a more predictive understanding of electronic excited-state phenomena and an essential step to the development of design rules for solar materials.



■ ELECTRON LOCALIZATION IN CHARGE TRANSFER EXCITED STATES

Energy migration and charge separation represent essential steps in molecularly based light-harvesting materials, be they natural^{1–3} or synthetic.^{4–6} Long range order and strong intermolecular coupling facilitate fast energy migration. Environmental disorder and solvation, as well as intramolecular distortion, disturb long-range order and suppress energy migration but facilitate charge separation. These variations in interaction strength also significantly influence the theoretical framework required to describe the resultant phenomena.^{4,7} The weak coupling regime dominates intermolecular energy transfer, but the conversion of excitation energy into chemical energy necessitates charge separation, a process that cannot be

described within the weak coupling regime. While Marcus theory provides a phenomenological framework for electron transfer reactions,^{8–10} we do not have the theoretical tools to predict electronic excited-state charge transfer phenomena with sufficient fidelity to be of practical value.

Charge transfer excited states in a high symmetry coordination complex have either an electron or a hole residing in one of many degenerate molecular orbitals. For the idealized degenerate case, coupling between degenerate molecular orbitals leads to delocalization of the excited state, while static and dynamic disorder will reduce the symmetry, eliminate the

Received: November 10, 2014

Published: March 19, 2015

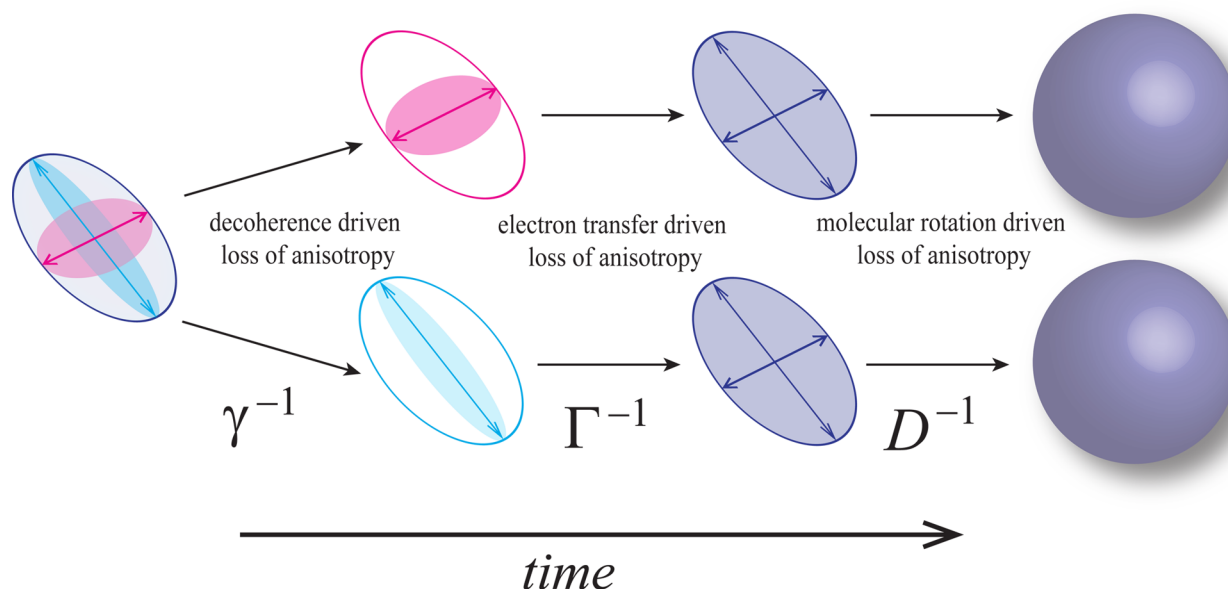


Figure 1. A schematic depiction of the electronic excited-state relaxation processes for a 2-fold degenerate system: γ is the rate of the decoherence, Γ is the rate of the incoherent electron transfer, and D is the rate of molecular rotation. This hierarchy of rates applies generally, but does not need to hold for all circumstances.

energetic degeneracy between electronic orbitals, and provide a mechanism for electron localization. For these reasons, the time-dependent spatial extent of charge transfer excited states in high symmetry coordination complexes provides a critical means of assessing how fundamental molecular properties and processes (coupling between degenerate electronic states, intramolecular symmetry breaking vibronic interactions, and intermolecular solvation driven symmetry breaking) control excited-state electronic structure and charge separation. The accessibility of charge transfer excited states to femtosecond resolution optical spectroscopy and these measurements to theoretical modeling has made them an important testing ground for how fundamental physical and chemical properties control charge separation and stabilization in electronic excited states.

These experimental and theoretical studies have emphasized the importance of time-resolved anisotropy for high symmetry molecules as a probe of the time dependent spatial extent of the electronic excited state.^{11–16} The time-resolved anisotropy measures the orientational memory of an optically generated excited state,¹⁷

$$r(t) = \frac{S_{\parallel}(t) - S_{\perp}(t)}{S_{\parallel}(t) + 2S_{\perp}(t)} \quad (1)$$

where S_{\parallel} represents the change in probe transmission induced by a pump pulse when the pump and probe beams have parallel linear polarizations, while S_{\perp} represents the signal with perpendicular linear polarizations for the pump and probe pulses. The spectral dependence of $r(t)$ will be discussed shortly. Under the most common circumstances, a low concentration of chromophores with nondegenerate excited states will have an anisotropy that ranges from 0.4 to 0, where the decay in the anisotropy results from the rotation of excited-state molecules.¹⁷ When the pump pulse excites degenerate states with orthogonal transition dipole moments, the initial value of the anisotropy reflects the symmetry of the molecule and the decay of the anisotropy reflects multiple dynamical

processes.^{11–16} Molecules with 3-fold degeneracy will have $r(0) = 1.0$, while molecules with 2-fold degeneracy will have $r(0) = 0.7$.¹³ A schematic of the relevant processes for 2-fold degenerate molecules appears in Figure 1. The dynamical phenomena that govern the loss of anisotropy for the 2-fold degenerate states can be expressed with three rates reflecting three distinct processes for an overdamped superposition of excited states,¹²

$$r(t) = \frac{1}{10}(1 + 3e^{-2\Gamma t} + 3e^{-\gamma t})e^{-6Dt} \quad (2)$$

Dephasing due to inter- and intramolecular fluctuations occurs with a γ rate and leads to localization of the charge transfer excited state to a single molecular orbital and reduction in anisotropy to $r = 0.4$. Incoherent electron transfer between degenerate localized charge transfer excited states occurs with a Γ rate and further reduces the anisotropy to $r = 0.1$ for 2-fold degenerate states. This assumes that the degenerate states have orthogonal transition dipole directions. Excited state bond rotation can also lead to changes in the anisotropy,^{18,19} though not for the charge transfer systems discussed in this Account. For dilute excitation, where excitation transfer between molecules does not occur, molecular rotation with the rate D causes the final loss of anisotropy.

Ruthenium tris-bipyridine, $[\text{Ru}(2,2'\text{-bipyridine})_3]^{2+}$,^{14–16} and tetraphenyl porphyrin¹² have been the molecular systems of choice for time-resolved studies of excited-state electron localization. In both systems, the molecular symmetry leads to 2-fold degenerate electronic excited states with orthogonal transition dipole moments. These studies have measured the polarization-dependent change in UV–visible probe absorption induced by the visible pump pulse. UV–visible pump–probe spectroscopy has three distinct sources of signal: a reduction in ground state absorption or ground state bleach (GSB), stimulated emission (SE) from electronic excited states back to the ground state, and new excited-state absorptions (ESA). The GSB and SE lead to an increase in probe light transmission, while the ESA reduces the signal transmission.

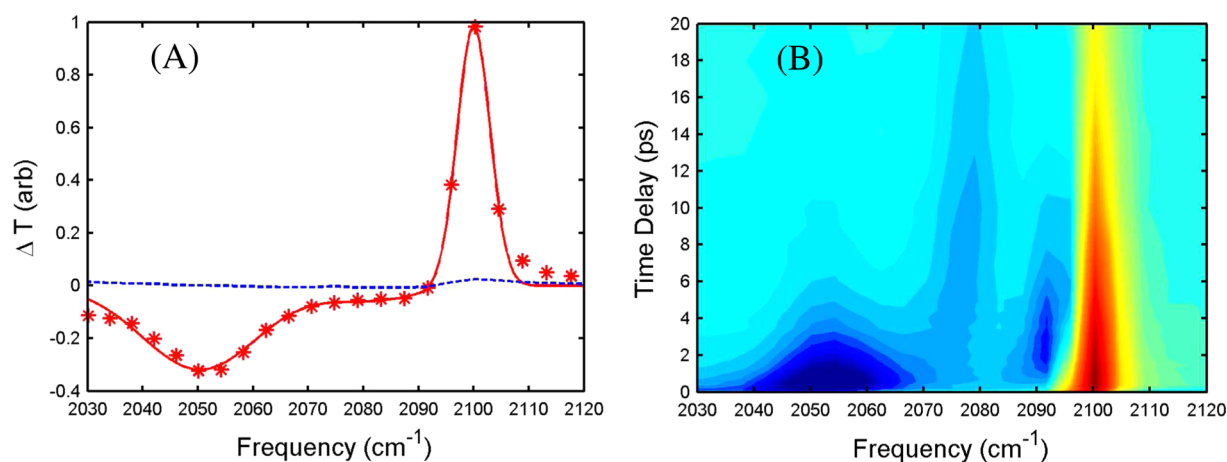


Figure 2. UV pump–mid-IR probe results for $[\text{Fe}(\text{CN})_6]^{3-}$ dissolved in dimethyl sulfoxide. (A) The isotropic (red points) and $S_{\parallel}-S_{\perp}$ difference (blue traces) transient spectra are shown for a 0.2 ps time delay. The solid red line is the fit of isotropic transient spectra. (B) Two-dimensional isotropic transient spectra as a function of mid-IR probe time delay and frequency. These figures are adapted with permission from Zhang et al., ref 24. Copyright 2012 American Chemical Society.

The biggest challenge occurs when the ESA spectrally overlaps with either the GSB or the SE. When signals of opposite sign spectrally overlap, a common occurrence, the anisotropy extracted from eq 1 can range from $-\infty$ to $+\infty$ making the measurement meaningless.

The contradictory interpretations of anisotropy measurements for the metal-to-ligand charge transfer (MLCT) excited state of $[\text{Ru}(2,2'\text{-bipyridine})_3]^{2+}$ highlight the challenges in interpreting time-resolved anisotropy measurements. Wallin et al. concluded from their measurements that the MLCT excited state delocalizes in less than a picosecond,¹⁶ while Malone and Kelley concluded that interligand hopping occurs with a 47 ps time constant.¹⁴ In a third study performed by Yeh et al., they observed optical dephasing on the 100 fs time scale, but did not report ultrafast interligand hopping of the MLCT excited state.¹⁵ These difficulties in experimental interpretation can be addressed, at least in part, by a change in experimental design.

Vibrational spectroscopy as a probe of electron localization and charge transfer has many attributes well suited to this problem. For an appropriately chosen molecule and vibrational probe, the anisotropic pump–probe signal can be placed in the molecular frame effectively. For instance, the first application of the method was able to determine the geometry of the CO bond to heme in myoglobin^{20,21} and has also been used to characterize the structure and dynamics of photoisomerization^{19,22} and the structural response of an enzyme to a photoexcited inhibitor.²³ We have used polarization-resolved UV pump mid-IR probe spectroscopy^{19–23} to study the electron localization dynamics of $\text{Fe}(\text{CN})_6^{3-}$.²⁴ We generate a ligand to metal charge transfer (LMCT) excited state and probe the electronic excited-state dynamics with the CN stretch absorption band with mid-IR pulses polarized parallel and perpendicular to the UV pump polarization. The CN-stretch vibration presents many interpretive advantages over UV–visible probing for tracking the dynamics of electronic excited states. The simplicity of vibrational line shapes allows us to clearly distinguish the ESA from the GSB signal, and the transient vibrational spectrum does not have a SE signal. The CN-stretching modes have transition dipole moments parallel to the CN bonding for both the ground and excited state, greatly simplifying the interpretation of the pump–probe anisotropy.

The experiment showed a variety of initially surprising results. The octahedral $\text{Fe}(\text{CN})_6^{3-}$ complex only has a 3-fold degenerate T_{1u} CN-stretching mode in the mid-IR absorption spectrum. As shown in Figure 2A, strong interligand electronic coupling in the LMCT excited state leads to electron hole delocalization. This preserves the octahedral symmetry and leads to a single T_{1u} CN-stretch ESA band at 2050 cm^{-1} with no anisotropy by a 0.2 ps time delay. With a solvent dependent rate, we observed that this single excited-state absorption converts to two ESA peaks appearing at 2079 and 2095 cm^{-1} with a 5 ps time constant. This can be seen in Figure 2B, which presents a contour plot of the full relaxation dynamics. The single excited-state absorption at short time delays and the absence of anisotropy demonstrate that the ligand hole in the LMCT electronic excited state hops very quickly from ligand to ligand, making the excited state look delocalized on the vibrational time scale. This indicates that the measurement lacks sufficient temporal resolution to observe the initial dephasing and intraligand charge transfer rates represented by γ and Γ in eq 2. The eventual appearance of two distinct vibrational transitions with the same rise and decay time constants shows that the ligand hole does eventually localize on a single ligand for sufficient time for the vibrational absorption spectrum to reflect the reduction in molecular symmetry associated with a localized LMCT excited state. As can be seen in Figure 2, the loss in symmetry causes two CN-stretch absorption peaks split by 20 cm^{-1} . Experimentally resolving the reduction in symmetry with vibrational spectroscopy requires roughly 1 ps, the period of a 20 cm^{-1} beat frequency. For hopping rates fast compared with 1 ps, the two transitions will motionally narrow into a single transition, making vibrational spectroscopy insensitive to the ligand hole localization. This highlights the core weakness of vibrational spectroscopy as a probe of photochemical dynamics; for small and moderate frequency shifts, the intrinsic time resolution of the measurement is usually limited to hundreds of femtoseconds, independent of the instrument response in the experiment.

Our measurements agree with the subpicosecond loss of anisotropy found for degenerate electronic excited states in tetraphenyl porphyrin by Hochstrasser and co-workers¹² and the degenerate MLCT excited state of $[\text{Ru}(2,2'\text{-bipyridine})_3]^{2+}$ by Hammerström and co-workers.¹⁶ We believe that the weight

of evidence supports very fast decoherence and electron hopping between equivalent excited states in room temperature solvent. Direct application of mid-IR anisotropy measurements to $[\text{Ru}(2,2'\text{-bipyridine})_3]^{2+}$ or tetraphenyl porphyrin would not easily clarify the situation, because these molecules lack vibrational transitions that can be easily mapped onto the charge transfer coordinates. The added value of vibrational anisotropy measurements usually requires the vibrational probe to be well described as a local mode where the vibrational transition dipole moment maps onto a critical molecular coordinate. Vibrational labeling with local vibrational modes, such as cyano groups, provides a chemical means of extending the value of vibrational anisotropy measurements.^{19,23,25,26}

MECHANISTIC STUDIES OF INTERSYSTEM CROSSING IN TRANSITION METAL COMPLEXES

A dynamical hierarchy has often been presumed to exist for the relaxation of electronic excited states in molecular systems, with intramolecular vibrational redistribution (IVR) preceding internal conversion, which in turn, precedes intersystem crossing. This hierarchy fails to describe excited-state dynamics in transition metal complexes; in point of fact, it would appear to be the exception rather than the rule,²⁷ with internal conversion and intersystem crossing often occurring on the same time scale as intramolecular vibrational redistribution. This general observation aligns with a more nuanced view of electronic excited-state dynamics, one where trajectories on excited-state potential energy surfaces that move through or near intersections between electronic excited states govern the rate of internal conversion and intersystem crossing.²⁸ Since vibrational motion and redistribution of vibrational energy control how molecules sample their excited-state potentials, the presumed separation of time scales for IVR, internal conversion, and intersystem crossing provides a poor starting point for rationalizing electronic excited-state dynamics.

The presence of metal centered excited states with distinct spin states represents a clear distinction between organic and inorganic molecular complexes. This proves particularly important for the excited-state dynamics of 3d transition metal complexes where the optically active excited states rarely correspond to the lowest energy excited states. This aspect of the energy levels of coordination complexes has long been appreciated since weak absorptions in the near IR due to symmetry forbidden d–d transitions can be seen at lower excitation energies than the charge transfer excitations that dominate the UV and visible absorption spectrum. However, the importance of these ligand field excited states in the relaxation of charge transfer excited states has taken longer to appreciate for both technical and scientific reasons. Scientifically, conventional wisdom presumed processes such as photoinduced spin crossover should proceed slowly because the conversion of a charge transfer excited state to a high spin ligand field excited state generally involves two active electrons, each of which must undergo internal conversion or intersystem crossing. Technically, assembling sufficiently robust evidence for the rate of photoinduced spin crossover progressed slowly because of the weight of evidence needed to supersede conventional wisdom.

Photoinduced spin crossover in polypyridal $\text{Fe}(\text{II})$ ^{27,29–39} has proven to be of particular importance because of the interest in using spin crossover materials in light triggered data storage³⁰ and iron based dyes as earth abundant light harvesters in dye sensitized solar cells.^{35,40,41} In both cases, the rate of

photoinduced spin crossover proves critical, since this rate controls the switching time on the one hand and competes with charge injection on the other. Figure 3 shows $[\text{Fe}(2,2'$

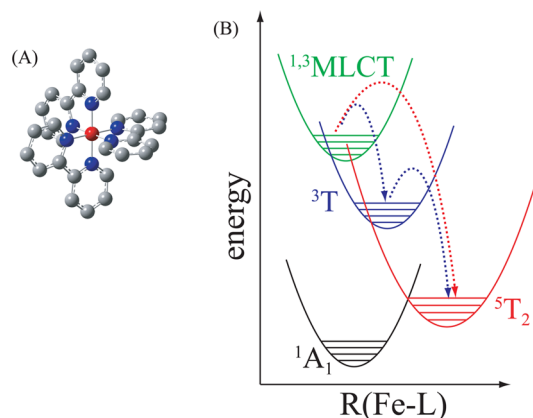


Figure 3. (A) Molecular structure of $[\text{Fe}(2,2'\text{-bipyridine})_3]^{2+}$ (red, Fe; blue, N; gray, C; H not shown). (B) A schematic drawing of the potential energy surfaces involved in the spin crossover dynamics. The figure shows two spin crossover pathways, one involving a triplet intermediate state (blue arrows) and one without a triplet intermediate state (red arrow). These figures are adapted with permission from Zhang et al., ref 46. Copyright 2014 Nature Publishing Group.

bipyridine)₃]²⁺, an archetypical spin crossover complex, along with the electron configurations associated with various electronic states and a schematic of how the Fe–N bond length varies for these distinct electronic states. Unlike many organic molecules, changes in spin state lead to significant changes in molecular geometry. This results from the metal–ligand antibonding character of the e_g levels only occupied in the high spin configurations. As shown schematically in Figure 3, and consistent with the theoretical calculations of de Graaf and Sousa,^{42–44} these large differences in structure can lead to energetic degeneracies between these distinct electronic states. If the electronic excited-state trajectories encounter these degeneracies, prompt nonadiabatic transitions between the degenerate states will occur, assuming there is sufficient electronic coupling. For spin crossover, this requires both vibronic and spin–orbit coupling. Formally atomic spin–orbit coupling does not apply, because the lower molecular symmetry does not conserve orbital angular momentum, but a change in spin state can occur if the electronic wave function also has a change of ± 1 angular node in analogy with spin–orbit coupling.⁴⁵

Initial picosecond and femtosecond resolution measurements indicated that spin crossover in polypyridal iron complexes occurred on a subpicosecond time scale,³⁴ but robust proof of this observation required numerous measurements with a variety of ultrafast methods.^{32,33,35,38,39,46} The characterization of photoinduced spin crossover dynamics took longer to acquire than many other photochemical phenomena because of the complexity of the phenomena and simultaneous evolution of the electronic, spin, and structural configuration. A long-standing difficulty has been the development of a general method for detecting spin state changes with femtosecond temporal resolution. While methods like electron paramagnetic resonance provide a sensitive probe of electronic spin moment, the intrinsic energy scale of the spin resonance process generally limits the time resolution from hundreds of

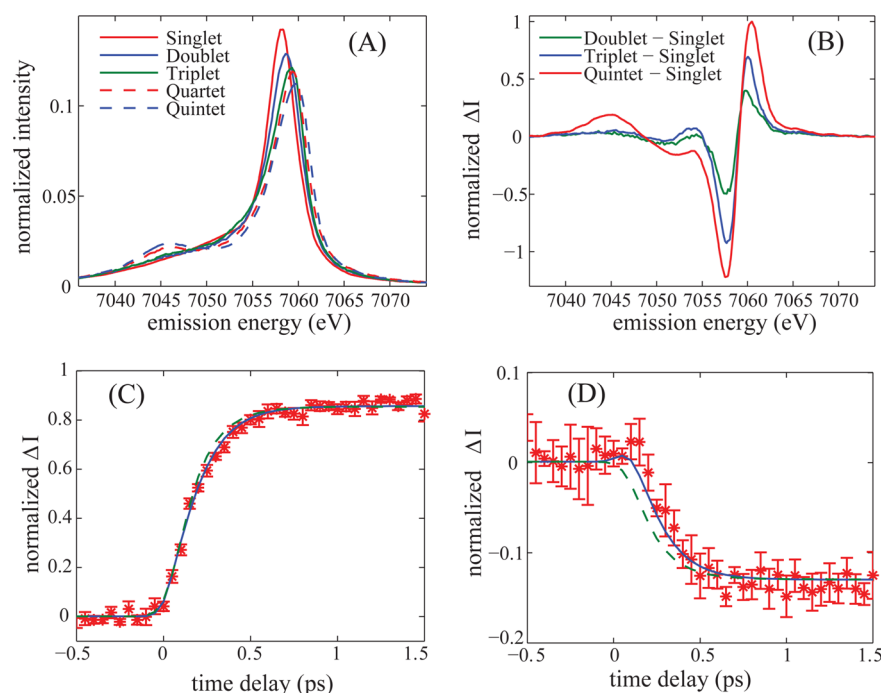


Figure 4. Spin-dependent iron $K\beta$ fluorescence spectra and time-dependent photoinduced iron $K\beta$ difference spectra and kinetic modeling of spin crossover dynamics. (A) The $K\beta$ fluorescence spectra of ground state iron complexes with different spin moments: singlet ($[\text{Fe}(2,2'\text{-bipyridine})_3]^{2+}$, red), doublet ($[\text{Fe}(2,2'\text{-bipyridine})_3]^{3+}$, blue), triplet (iron(II) phthalocyanine, green), quartet (iron(III) phthalocyanine chloride, red dashed), and quintet ($[\text{Fe}(\text{phenanthroline})_2(\text{NCS})_2]$, blue dashed). (B) Model complex difference spectra for the ${}^1{}^3\text{MLCT}$, ${}^3\text{T}$, and ${}^5\text{T}_2$ excited states constructed by subtracting the singlet model complex spectrum from the doublet, triplet, and quintet model complex spectra shown in panel A. (C, D) Time-dependent optically induced difference spectra measured at a $K\beta$ fluorescence energy of 7061 eV (C) and 7054 eV (D) for $[\text{Fe}(2,2'\text{-bipyridine})_3]^{2+}$ (red stars), as well as the best fit achieved for kinetic models with (blue) or without (green dashed) a ${}^3\text{T}$ transient. The error bars in panels C and D reflect the standard error for the difference signal determined from six independent measurements. These figures are adapted with permission from Zhang et al., ref 46. Copyright 2014 Nature Publishing Group.

picoseconds to nanoseconds. X-ray spectroscopy,⁴⁷ particularly hard X-ray fluorescence^{46,48–51} and soft X-ray absorption spectroscopy^{37,38,52} for 3d transition metals, provide sensitive measures of the metal spin state and have intrinsic time resolution on the single femtosecond time scale as reflected by the absorption and fluorescence line widths.⁵³ The value of new and complementary experimental methods becomes even more critical as the objective transitions from measuring the rate of spin crossover to determining the mechanism of spin crossover and controlling the excited-state spin dynamics.

We have focused our effort on the development of Fe $K\beta$ fluorescence spectroscopy as a probe of spin dynamics,⁴⁶ though Fe 2p absorption spectroscopy^{37,38} and Fe $K\alpha$ fluorescence^{50,51} have also proven to be valuable probes of excited-state spin dynamics. Ionization of the Fe 1s orbital with a hard X-ray photon above the Fe 1s ionization potential of 7120 eV leads to X-ray fluorescence. Fe $K\beta$ fluorescence involves 3p filling of the 1s hole. The strong exchange interaction between the 3d electrons and the hole in the 3p level created by fluorescence makes the $K\beta$ fluorescence spectrum sensitive to the 3d spin moment.^{47,49,54} This sensitivity can be seen in Figure 4A, where the Fe $K\beta$ fluorescence spectrum for a variety of Fe compounds with distinct spin moments has been plotted. The dominant source of spectral variation results from variation in spin state, making $K\beta$ fluorescence an excellent probe of spin dynamics.

The predominant influence of spin on the $K\beta$ spectrum has enabled us to use electronic ground state spectra as models for excited-state changes in Fe spin and charge due to the change in spin that accompanies a change in oxidation state.⁴⁶ Figure

4B shows the model difference spectra associated with the distinct excited state that could participate in photoinduced spin crossover. Before discussing the time dependent difference signals measured for $[\text{Fe}(2,2'\text{-bipyridine})_3]^{2+}$, the limitations of using electronic ground state $K\beta$ spectra to model electronic excited-state spectra warrant discussion. A variety of measurements and calculated spectra have demonstrated that the $K\beta$ spectrum shows little sensitivity to molecular symmetry for equal spin states,^{46,49} but the covalency of the metal–ligand bond does have an impact on the spectrum.⁵⁵ This has been demonstrated most clearly for iron complexes at the extremes of metal–ligand covalency.⁵⁵ For instance, strongly covalent iron sulfur complexes appear to have smaller effective spin moments than those for highly ionic iron fluoride. This spectral variation results from the delocalization of the spin density, while the $K\beta$ spectrum only reflects the Fe contribution to the spin moment. This aspect of the $K\beta$ fluorescence spectroscopy adds to the information content of the technique but also means that molecules with similar coordination bonding need to be chosen to model excited-state spin dynamics.

The sensitivity of the $K\beta$ fluorescence spectra to the iron spin moment enables the spin crossover mechanism to be monitored. While the subpicosecond rate of spin crossover in multiple iron polypyridal complexes has been established by a large number of measurements and methods,^{32,33,35,38,39} the mechanism for the process has proven more difficult to determine. Whether the MLCT state decays directly to the high spin quintet ligand field excited state (${}^5\text{T}_2$)^{32,33} or through a triplet ligand field excited-state (${}^3\text{T}$) transient^{30,31,46} has been a question of central mechanistic importance. Chergui et al. have

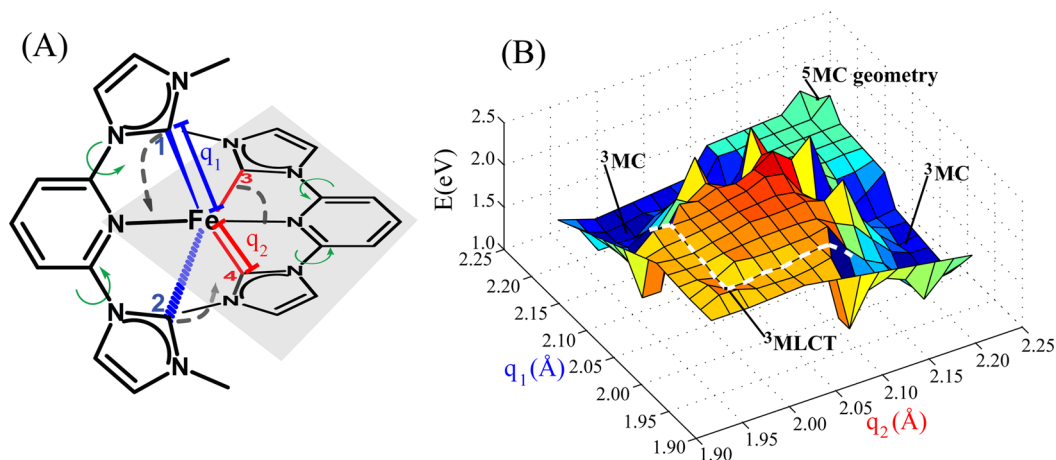


Figure 5. (A) Structure of $[\text{Fe}(\text{CNC})_2]^{2+}$ ($\text{CNC} = 2,6\text{-bis}(3\text{-methylimidazole-1-ylidene})\text{pyridine}$) and geometrical structure parameters. (B) $[\text{Fe}(\text{CNC})_2]^{2+}$ potential energy surface between the ${}^3\text{MLCT}$ and metal centered quintet (${}^5\text{MC}$) geometries, where the white dotted path is the lowest-energy path between the ${}^3\text{MLCT}$ and the metal centered triplet (${}^3\text{MC}$) states. ${}^5\text{MC}$ and ${}^3\text{MC}$ play analogous roles in $[\text{Fe}(\text{CNC})_2]^{2+}$ as ${}^3\text{T}$ and ${}^5\text{T}_2$ do for $[\text{Fe}(2,2'\text{-bipyridine})_3]^{2+}$. These figures are adapted with permission from Fredin et al., ref 57. Copyright 2014 American Chemical Society.

used UV–visible transient absorption,^{33,56} time-resolved luminescence,³³ and time-resolved iron K-edge XANES³² to characterize the spin crossover dynamics of $[\text{Fe}(2,2'\text{-bipyridine})_3]^{2+}$. They concluded from the time-resolved luminescence studies that the optically excited ${}^1\text{MLCT}$ state decayed to a ${}^3\text{MLCT}$ with a ~ 30 fs time constant. With a combination of UV–visible and Fe K-edge X-ray absorption measurements, they concluded that the rate of ${}^3\text{MLCT}$ decay matched the rate of ${}^5\text{T}_2$ formation, leading them to conclude that the ${}^3\text{MLCT}$ excited state converts directly to the ${}^5\text{T}_2$ excited state.³² We have drawn the opposite conclusion from our femtosecond resolution visible pump $K\beta$ fluorescence probe measurements,⁴⁶ where the transient signal provides strong evidence for spin crossover proceeding through a triplet transient.

Figure 4C,D shows transient difference spectra for $[\text{Fe}(2,2'\text{-bipyridine})_3]^{2+}$. The distinct features of the ${}^3\text{T}$ difference spectrum allow the potential presence of a ${}^3\text{T}$ transient state to be distinguished from ${}^{1,3}\text{MLCT}$ and ${}^5\text{T}_2$ excited states in the transient difference spectra. We fit the time-dependent difference spectra to two distinct models: one where the ${}^{1,3}\text{MLCT}$ decays directly to a ${}^5\text{T}_2$ excited state and one where the ${}^{1,3}\text{MLCT}$ relaxes to the ${}^5\text{T}_2$ state via a ${}^3\text{T}$ transient. Statistical analysis allows us to reject the direct MLCT to ${}^5\text{T}_2$ mechanism with greater than 95% confidence. Figure 4C,D shows the time-dependent difference signal measured at two X-ray fluorescence energies, 7061 eV, where the difference signal is largest, and 7054 eV, where the triplet model complex has a spectral signature clearly distinct from the ${}^{1,3}\text{MLCT}$ and ${}^5\text{T}_2$ states. In the absence of a triplet transient, the strong increase in fluorescence signal at 7061 eV also generates a fast decrease in signal at 7054 eV, while the measurement shows a delay in the decrease in signal at 7054 eV relative to rise at 7061 eV. With the triplet transient, the signal changes at both 7061 and 7054 eV consistent with the experimental results.

The calculations of de Graaf and Sousa indicate that both the direct ${}^{1,3}\text{MLCT} \rightarrow {}^5\text{T}_2$ and the sequential ${}^{1,3}\text{MLCT} \rightarrow {}^3\text{T} \rightarrow {}^5\text{T}_2$ mechanisms provide energetically feasible reaction pathways with minimal reaction barriers.^{42–44} The relative strength of the coupling between the states likely determines which pathway dominates. We conclude that the sequential relaxation

occurs more promptly than the direct crossover from the ${}^{1,3}\text{MLCT}$ to the ${}^5\text{T}_2$ excited state because the sequential transition involves single electronic transitions coupled by a spin–orbit operator, while the direct transition involves the simultaneous transition of two distinct electrons on two centers and cannot occur with the first-order spin–orbit operator. The theoretical study of Sousa et al. supports this conclusion,⁴² where they calculated significantly faster spin crossover for the sequential mechanism than the direct mechanism.

Time resolved X-ray spectroscopy measurements^{38,46} have significantly clarified the electronic states involved in photo-induced spin crossover, but this only represents half of the mechanism. A mechanistic understanding also requires a detailed understanding of the vibrational motions involved in the nonadiabatic transitions between the critical electronic states involved in spin crossover.^{57,58} The desire to control or eliminate spin crossover for photocatalytic and photovoltaic applications accentuates the need to identify the vibrations involved in spin crossover. Consistent with Figure 3, the Fe–N bond length receives the most attention. The dynamics of this bond expansion have been directly tracked using Fe K-edge XANES,^{32,39} X-ray scattering,⁵¹ and quantum chemical calculations.^{42–44} This bond expansion corresponds to the vibrational motion that undergoes the largest reorganization during spin crossover and likely plays a critical role in the transition from ${}^3\text{T}$ to ${}^5\text{T}_2$, as indicated by the potential energy surfaces calculated by de Graaf and Sousa.^{42–44} The importance of the Fe–N stretching motion to the transition between the MLCT and the ${}^3\text{T}$ excited states seems much less apparent. Quantum chemical calculations show little change in the Fe–N bond lengths between the singlet ground state and the MLCT excited state.^{43,44} Given that the formation of the ${}^3\text{T}$ transient controls the rate of spin crossover, determining the reaction coordinate vibrations for this step represents a critical step toward controlling MLCT excited-state dynamics in coordination complexes.

The inability of Fe–N bond expansion alone to explain the electronic excited-state relaxation warrants emphasis. For spin crossover $3d^6$ systems with pseudo-octahedral symmetry, metal centered triplet states have a single electron in the degenerate e_g level. This makes the system Jahn–Teller or

pseudo-Jahn–Teller active and should lead to a tetragonal distortion of the molecular symmetry. This effect has been observed in quantum chemical studies of the excited-state structure of iron carbene complexes,^{57,59} as shown in Figure 5, but has not been investigated in theoretical studies of $[\text{Fe}(2,2'\text{-bipyridine})_3]^{2+}$ photoinduced spin crossover. For the iron carbene complex shown in Figure 5A, the triplet state only involves elongation of the Fe–C bonds in blue (q_1) or equivalently red (q_2) to stabilize the metal centered triplet state, while the quintet state undergoes symmetric elongation of both q_1 and q_2 . Inner-shell torsional dynamics could also be significant. For bi- and tridentate ligands changes in Fe–N bond length also leads to distortions in the N–Fe–N bond angles.⁵⁸ Generally this means that changes in N–Fe–N bond angles accompany changes in Fe–N bond length. To date, the influence of these coupled structural motions on the excited-state electron dynamics involved in spin crossover has not been fully characterized either experimentally or theoretically.

The ability to track the spin state of metal centered excited states also provides the opportunity to investigate the role of spin in catalytic mechanisms. Spin state changes in the catalytic mechanisms of 3d transition metal catalysts have been proposed for a variety of reactions including ligand binding to $\text{Fe}(\text{CO})_4$ ^{60–64} and Ni porphyrins,⁶⁵ as well as bond activation by heme and non-heme iron-oxo complexes.⁶⁶ The generation of metastable spin states with optical excitation provides a novel approach to investigating the influence of the metal center spin state on bond activation.

■ PROSPECTIVE

Mixed ligation, variation in ligand field strength, and ligand coordination number all provide means to manipulate the nuclear and electronic structure of coordination complexes. Mature methods for synthesizing, characterizing, and simulating the electronic ground state properties of diverse coordination complexes exist in abundance. Methods for characterizing and simulating the electronic excited-state properties of these compounds remain comparatively rudimentary, but advances in computational power and methodology, as well as ultrafast laser technology, give reason for hope that our ability to characterize and understand electronic excited-state properties in coordination chemistry should advance quickly. X-ray free electron lasers, capable of generating few femtosecond duration pulses with roughly millijoule energies, represent the most compelling experimental advance relevant to the study of the electronic excited-state properties of coordination complexes. While hard X-ray fluorescence measurements have been emphasized in this Account,^{46,50,51,67} a variety of ultrafast resolution X-ray scattering and spectroscopy methods have been demonstrated.^{39,68–71} Unlike prior studies utilizing femtosecond laser plasmas or strong field laser manipulation of X-ray synchrotrons, the high flux of femtosecond duration X-ray laser sources no longer requires heroic effort to achieve limited signal quality. Despite the excitement, the results remain largely incremental. Genuine impact will require collaboration between scientists with expertise in molecular synthesis, quantum dynamics simulations, and experimental measurement. Only through coordinated effort will we reach the true objective of understanding how ground state molecular structure dictates electronic excited-state properties.

■ AUTHOR INFORMATION

Corresponding Author

*E-mail: kgaffney@slac.stanford.edu.

Notes

The authors declare no competing financial interest.

Biographies

Wenkai Zhang was born in Shanxi province, China in 1978. He received his B.S. in Chemistry from University of Science and Technology of China in 2001, and his Ph.D. in Physical Chemistry from the Institute of Chemistry, the Chinese Academy of Sciences under the direction of Professor Hongfei Wang in 2007. Wenkai Zhang did his postdoctoral research with Professor Haw Yang at University of California, Berkeley, in 2007, and with Professor Kelly Gaffney at the Photon Science at Stanford University and the SLAC National Accelerator Laboratory from 2007 to 2013. Now, he is continuing his postdoctoral research at the Ultrafast Optical Processes Laboratory, an NIH Biomedical Technology Research Center, directed by Professor Feng Gai at the University of Pennsylvania.

Kelly Gaffney grew up in Seattle, WA, his place of birth in 1970. He attended The Evergreen State College where he studied environmental chemistry and graduated in 1993. After two years as an industrial analytical chemist, Kelly Gaffney began his Ph.D. studies at the University of California, Berkeley, Chemistry Department under the direction of Professor Charles Harris. After graduating in 2001, Dr. Gaffney joined the research group of Professor Michael Fayer at Stanford University, before joining the Photon Science faculty at Stanford University and the SLAC National Accelerator Laboratory in 2004. He currently holds the rank of associate professor and also serves as the Director of the Stanford Synchrotron Radiation Lightsource.

■ ACKNOWLEDGMENTS

The authors thank the numerous collaborators that contributed to the work in this Account and acknowledge support from the AMOS program within the Chemical Sciences, Geosciences, and Biosciences Division of the Office of Basic Energy Sciences, Office of Science, U.S. Department of Energy.

■ REFERENCES

- (1) van Grondelle, R.; Dekker, J. P.; Gillbro, T.; Sundstrom, V. Energy-transfer and trapping in photosynthesis. *Biochim. Biophys. Acta, Bioenerg.* **1994**, *1187*, 1–65.
- (2) Scholes, G. D.; Fleming, G. R. On the mechanism of light harvesting in photosynthetic purple bacteria: B800 to B850 energy transfer. *J. Phys. Chem. B* **2000**, *104*, 1854–1868.
- (3) Engel, G. S.; Calhoun, T. R.; Read, E. L.; Ahn, T. K.; Mancal, T.; Cheng, Y. C.; Blankenship, R. E.; Fleming, G. R. Evidence for wavelike energy transfer through quantum coherence in photosynthetic systems. *Nature* **2007**, *446*, 782–786.
- (4) Thompson, A. L.; Gaab, K. M.; Xu, J. J.; Bardeen, C. J.; Martinez, T. J. Variable electronic coupling in phenylacetylene dendrimers: The role of Förster, Dexter, and charge-transfer interactions. *J. Phys. Chem. A* **2004**, *108*, 671–682.
- (5) Collini, E.; Scholes, G. D. Coherent Intrachain Energy Migration in a Conjugated Polymer at Room Temperature. *Science* **2009**, *323*, 369–373.
- (6) Wasielewski, M. R. Energy, charge, and spin transport in molecules and self-assembled nanostructures inspired by photosynthesis. *J. Org. Chem.* **2006**, *71*, 5051–5066.
- (7) Fernandez, E.; Blancafort, L.; Olivucci, M.; Robb, M. A. Intramolecular electron transfer: Independent (ground state) adiabatic

(chemical) and nonadiabatic reaction pathways in bis(hydrazine) radical cations. *J. Am. Chem. Soc.* **2000**, *122*, 7528–7533.

(8) Barbara, P.; Meyer, T.; Ratner, M. Contemporary issues in electron transfer research. *J. Phys. Chem.* **1996**, *100*, 13148–13168.

(9) Brunschwig, B. S.; Creutz, C.; Sutin, N. Optical transitions of symmetrical mixed-valence systems in the Class II-III transition regime. *Chem. Soc. Rev.* **2002**, *31*, 168–184.

(10) Demadis, K. D.; Hartshorn, C. M.; Meyer, T. J. The localized-to-delocalized transition in mixed-valence chemistry. *Chem. Rev.* **2001**, *101*, 2655–2685.

(11) Knox, R. S.; Gulen, D. Theory of polarized fluorescence from molecular pairs - Forster transfer at large electronic coupling. *Photochem. Photobiol.* **1993**, *57*, 40–43.

(12) Galli, C.; Wynne, K.; Lecours, S. M.; Therien, M. J.; Hochstrasser, R. M. Direct measurement of electronic dephasing using anisotropy. *Chem. Phys. Lett.* **1993**, *206*, 493–499.

(13) Wynne, K.; Hochstrasser, R. M. Anisotropy as an ultrafast probe of electronic coherence in degenerate systems exhibiting Raman-scattering, fluorescence, transient absorption, and chemical-reactions. *J. Raman Spectrosc.* **1995**, *26*, 561–569.

(14) Malone, R. A.; Kelley, D. F. Interligand electron-transfer and transition-state dynamics in Ru(II) trisbipyridine. *J. Chem. Phys.* **1991**, *95*, 8970–8976.

(15) Yeh, A. T.; Shank, C. V.; McCusker, J. K. Ultrafast electron localization dynamics following photo-induced charge transfer. *Science* **2000**, *289*, 935–938.

(16) Wallin, S.; Davidsson, J.; Modin, J.; Hammarstrom, L. Femtosecond transient absorption anisotropy study on Ru(bpy)(3) (2+) and Ru(bpy)(py)(4) (2+). Ultrafast interligand randomization of the MLCT state. *J. Phys. Chem. A* **2005**, *109*, 4697–4704.

(17) Berne, B. J.; Pecora, R. *Dynamic Light Scattering*; Dover: Mineola, NY, 2000.

(18) Sension, R. J.; Repinec, S. T.; Szarka, A. Z.; Hochstrasser, R. M. Femtosecond laser studies of the cis-stilbene photoisomerization reactions. *J. Chem. Phys.* **1993**, *98*, 6291–6315.

(19) Zhang, W. K.; Lan, Z. G.; Sun, Z.; Gaffney, K. J. Resolving photo-induced twisted intramolecular charge transfer with vibrational anisotropy and TDDFT. *J. Phys. Chem. B* **2012**, *116*, 11527–11536.

(20) Moore, J. N.; Hansen, P. A.; Hochstrasser, R. M. Iron carbonyl bond geometries of carboxymyoglobin and carboxyhemoglobin in solution determined by picosecond time-resolved infrared-spectroscopy. *Proc. Natl. Acad. Sci. U. S. A.* **1988**, *85*, 5062–5066.

(21) Lim, M.; Jackson, T. A.; Anfinsen, P. A. Binding of Co to myoglobin from a heme pocket docking site to form nearly linear Fe-C-O. *Science* **1995**, *269*, 962–966.

(22) Heyne, K.; Mohammed, O. F.; Usman, A.; Dreyer, J.; Nibbering, E. T. J.; Cusanovich, M. A. Structural evolution of the chromophore in the primary stages of trans/cis isomerization in photoactive yellow protein. *J. Am. Chem. Soc.* **2005**, *127*, 18100–18106.

(23) Jha, S. K.; Ji, M. B.; Gaffney, K. J.; Boxer, S. G. Direct measurement of the protein response to an electrostatic perturbation that mimics the catalytic cycle in ketosteroid isomerase. *Proc. Natl. Acad. Sci. U. S. A.* **2011**, *108*, 16612–16617.

(24) Zhang, W. K.; Ji, M. B.; Sun, Z.; Gaffney, K. J. Dynamics of solvent-mediated electron localization in electronically excited hexacyanoferrate(III). *J. Am. Chem. Soc.* **2012**, *134*, 2581–2588.

(25) Waegle, M. M.; Culik, R. M.; Gai, F. Site-specific spectroscopic reporters of the local electric field, hydration, structure, and dynamics of biomolecules. *J. Phys. Chem. Lett.* **2011**, *2*, 2598–2609.

(26) Levinson, N. M.; Fried, S. D.; Boxer, S. G. Solvent-induced infrared frequency shifts in aromatic nitriles are quantitatively described by the vibrational Stark effect. *J. Phys. Chem. B* **2012**, *116*, 10470–10476.

(27) Chergui, M. On the interplay between charge, spin and structural dynamics in transition metal complexes. *Dalton Trans.* **2012**, *41*, 13022–13029.

(28) Levine, B. G.; Martinez, T. J. Isomerization through conical intersections. *Annu. Rev. Phys. Chem.* **2007**, *58*, 613–634.

(29) Creutz, C.; Chou, M.; Netzel, T. L.; Okumura, M.; Sutin, N. Lifetimes, spectra, and quenching of the excited-states of polypyridine complexes of iron(II), ruthenium(II), and osmium(II). *J. Am. Chem. Soc.* **1980**, *102*, 1309–1319.

(30) Gutlich, P.; Goodwin, H. A. Spin crossover - An overall perspective. In *Spin Crossover in Transition Metal Compounds I*; Gutlich, P., Goodwin, H. A., Eds.; Springer-Verlag: Berlin, 2004; Vol. 233, pp 1–47.

(31) Hauser, A. Intersystem crossing in the Fe(PTZ)₆ (BF₄)₂ spin crossover system (PTZ = 1-propyltetrazole). *J. Chem. Phys.* **1991**, *94*, 2741–2748.

(32) Bressler, C.; Milne, C.; Pham, V. T.; ElNahas, A.; van der Veen, R. M.; Gawelda, W.; Johnson, S.; Beaud, P.; Grolimund, D.; Kaiser, M.; Borca, C. N.; Ingold, G.; Abela, R.; Chergui, M. Femtosecond XANES study of the light-induced spin crossover dynamics in an iron(II) complex. *Science* **2009**, *323*, 489–492.

(33) Gawelda, W.; Cannizzo, A.; Pham, V. T.; van Mourik, F.; Bressler, C.; Chergui, M. Ultrafast nonadiabatic dynamics of [Fe(II)(bpy)₃]²⁺ in solution. *J. Am. Chem. Soc.* **2007**, *129*, 8199–8206.

(34) McCusker, J. K.; Walda, K. N.; Dunn, R. C.; Simon, J. D.; Magde, D.; Hendrickson, D. N. Subpicosecond ¹MLCT-⁵T₂ Intersystem Crossing of Low-Spin Polypyridyl Ferrous Complexes. *J. Am. Chem. Soc.* **1993**, *115*, 298–307.

(35) Monat, J. E.; McCusker, J. K. Femtosecond excited-state dynamics of an iron(II) polypyridyl solar cell sensitizer model. *J. Am. Chem. Soc.* **2000**, *122*, 4092–4097.

(36) Khalil, M.; Marcus, M. A.; Smeigh, A. L.; McCusker, J. K.; Chong, H. H. W.; Schoenlein, R. W. Picosecond X-ray absorption spectroscopy of a photoinduced iron(II) spin crossover reaction in solution. *J. Phys. Chem. A* **2006**, *110*, 38–44.

(37) Huse, N.; Kim, T. K.; Jamula, L.; McCusker, J. K.; de Groot, F. M. F.; Schoenlein, R. W. Photo-induced spin-state conversion in solvated transition metal complexes probed via time-resolved soft X-ray spectroscopy. *J. Am. Chem. Soc.* **2010**, *132*, 6809–6816.

(38) Huse, N.; Cho, H.; Hong, K.; Jamula, L.; de Groot, F. M. F.; Kim, T. K.; McCusker, J. K.; Schoenlein, R. W. Femtosecond soft X-ray spectroscopy of solvated transition-metal complexes: Deciphering the interplay of electronic and structural dynamics. *J. Phys. Chem. Lett.* **2011**, *2*, 880–884.

(39) Lemke, H. T.; Bressler, C.; Chen, L. X.; Fritz, D. M.; Gaffney, K. J.; Galler, A.; Gawelda, W.; Haldrup, K.; Hartsock, R. W.; Ihee, H.; Kim, J.; Kim, K. H.; Lee, J. H.; Nielsen, M. M.; Stickrath, A. B.; Zhang, W. K.; Zhu, D. L.; Cammarata, M. Femtosecond X-ray absorption spectroscopy at a hard X-ray free electron laser: Application to spin crossover dynamics. *J. Phys. Chem. A* **2013**, *117*, 735–740.

(40) Ferrere, S.; Gregg, B. A. Photosensitization of TiO₂ by Fe-II(2,2'-bipyridine-4,4'-dicarboxylic acid)₂(CN)₂: Band selective electron injection from ultra-short-lived excited states. *J. Am. Chem. Soc.* **1998**, *120*, 843–844.

(41) Yang, M.; Thompson, D. W.; Meyer, G. J. Charge-transfer studies of iron cyano compounds bound to nanocrystalline TiO₂ surfaces. *Inorg. Chem.* **2002**, *41*, 1254–1262.

(42) Sousa, C.; de Graaf, C.; Rudavskiy, A.; Broer, R.; Tatchen, J.; Etinski, M.; Marian, C. M. Ultrafast deactivation mechanism of the excited singlet in the light-induced spin crossover of [Fe(2,2'-bipyridine)₃]²⁺. *Chem.—Eur. J.* **2013**, *19*, 17541–17551.

(43) de Graaf, C.; Sousa, C. On the role of the metal-to-ligand charge transfer states in the light-induced spin crossover in Fe-II(bpy)₃. *Int. J. Quantum Chem.* **2011**, *111*, 3385–3393.

(44) de Graaf, C.; Sousa, C. Study of the light-induced spin crossover process of the [Fe(II)(bpy)₃]²⁺ complex. *Chem.—Eur. J.* **2010**, *16*, 4550–4556.

(45) Marian, C. M. Spin-orbit coupling and intersystem crossing in molecules. *Wiley Interdiscip. Rev.: Comput. Mol. Sci.* **2012**, *2*, 187–203.

(46) Zhang, W. K.; Alonso-Mori, R.; Bergmann, U.; Bressler, C.; Chollet, M.; Galler, A.; Gawelda, W.; Hadt, R. G.; Hartsock, R. W.; Kroll, T.; Kjaer, K. S.; Kubicek, K.; Lemke, H. T.; Liang, H. W.; Meyer, D. A.; Nielsen, M. M.; Purser, C.; Robinson, J. S.; Solomon, E. I.; Sun, Z.; Sokaras, D.; Van Driel, T. B.; Vanko, G.; Weng, T. C.; Zhu, D.;

Gaffney, K. J. Tracking excited state charge and spin dynamics in iron coordination complexes. *Nature* **2014**, *509*, 345–348.

(47) de Groot, F. Multiplet effects in X-ray spectroscopy. *Coord. Chem. Rev.* **2005**, *249*, 31–63.

(48) Glatzel, P.; Bergmann, U. High resolution 1s core hole X-ray spectroscopy in 3d transition metal complexes - electronic and structural information. *Coord. Chem. Rev.* **2005**, *249*, 65–95.

(49) Vanko, G.; Neisius, T.; Molnar, G.; Renz, F.; Karpati, S.; Shukla, A.; de Groot, F. M. F. Probing the 3d spin momentum with X-ray emission spectroscopy: The case of molecular-spin transitions. *J. Phys. Chem. B* **2006**, *110*, 11647–11653.

(50) Vanko, G.; Glatzel, P.; Pham, V. T.; Abela, R.; Grolimund, D.; Borca, C. N.; Johnson, S. L.; Milne, C. J.; Bressler, C. Picosecond time-resolved X-ray emission spectroscopy: Ultrafast spin-state determination in an iron complex. *Angew. Chem., Int. Ed.* **2010**, *49*, 5910–5912.

(51) Haldrup, K.; Vanko, G.; Gawelda, W.; Galler, A.; Doumy, G.; March, A. M.; Kanter, E. P.; Bordage, A.; Dohn, A.; van Driel, T. B.; Kjaer, K. S.; Lemke, H. T.; Canton, S. E.; Uhlig, J.; Sundstrom, V.; Young, L.; Southworth, S. H.; Nielsen, M. M.; Bressler, C. Guest-host interactions investigated by time-resolved X-ray spectroscopies and scattering at MHz rates: Solvation dynamics and photoinduced spin transition in aqueous $[\text{Fe}(\text{bipy})_3]^{2+}$. *J. Phys. Chem. A* **2012**, *116*, 9878–9887.

(52) Josefsson, I.; Kunnus, K.; Schreck, S.; Fohlich, A.; de Groot, F.; Wernet, P.; Odellius, M. Ab initio calculations of X-ray spectra: Atomic multiplet and molecular orbital effects in a multiconfigurational SCF approach to the L-edge spectra of transition metal complexes. *J. Phys. Chem. Lett.* **2012**, *3*, 3565–3570.

(53) Krause, M. O.; Oliver, J. H. Natural widths of atomic K and L levels, K-alpha X-Ray lines and several KLL Auger lines. *J. Phys. Chem. Ref. Data* **1979**, *8*, 329–338.

(54) Lee, N.; Petrenko, T.; Bergmann, U.; Neese, F.; DeBeer, S. Probing valence orbital composition with iron K β X-ray emission spectroscopy. *J. Am. Chem. Soc.* **2010**, *132*, 9715–9727.

(55) Pollock, C. J.; Delgado-Jaime, M. U.; Atanasov, M.; Neese, F.; DeBeer, S. K β mainline X-ray emission spectroscopy as an experimental probe of metal-ligand covalency. *J. Am. Chem. Soc.* **2014**, *136*, 9453–9463.

(56) Consani, C.; Premont-Schwarz, M.; ElNahhas, A.; Bressler, C.; van Mourik, F.; Cannizzo, A.; Chergui, M. Vibrational coherences and relaxation in the high-spin state of aqueous $[\text{Fe-II}(\text{bpy})_3]^{2+}$. *Angew. Chem., Int. Ed.* **2009**, *48*, 7184–7187.

(57) Fredin, L. A.; Papai, M.; Rozsalyi, E.; Vanko, G.; Warnmark, K.; Sundstrom, V.; Persson, P. Exceptional excited-state lifetime of an iron(II)-N-heterocyclic carbene complex explained. *J. Phys. Chem. Lett.* **2014**, *5*, 2066–2071.

(58) Alvarez, S. Relationships between temperature, magnetic moment, and continuous symmetry measures in spin crossover complexes. *J. Am. Chem. Soc.* **2003**, *125*, 6795–6802.

(59) Liu, Y. Z.; Harlang, T.; Canton, S. E.; Chabera, P.; Suarez-Alcantara, K.; Fleckhaus, A.; Vithanage, D. A.; Goransson, E.; Corani, A.; Lomoth, R.; Sundstrom, V.; Warnmark, K. Towards longer-lived metal-to-ligand charge transfer states of iron(II) complexes: An N-heterocyclic carbene approach. *Chem. Commun.* **2013**, *49*, 6412–6414.

(60) Besora, M.; Carreon-Macedo, J.-L.; Cowan, A. J.; George, M. W.; Harvey, J. N.; Portius, P.; Ronayne, K. L.; Sun, X.-Z.; Towrie, M. A combined theoretical and experimental study on the role of spin states in the chemistry of $\text{Fe}(\text{CO})_5$ photoproducts. *J. Am. Chem. Soc.* **2009**, *131*, 3583–3592.

(61) Harvey, J. N. Understanding the kinetics of spin-forbidden chemical reactions. *Phys. Chem. Chem. Phys.* **2007**, *9*, 331–343.

(62) Poliakov, M.; Turner, J. J. The structure of $\text{Fe}(\text{CO})_4$ - An important new chapter in a long-running story. *Angew. Chem., Int. Ed.* **2001**, *40*, 2809–2812.

(63) Snee, P. T.; Payne, C. K.; Kotz, K. T.; Yang, H.; Harris, C. B. Triplet organometallic reactivity under ambient conditions: An ultrafast UV pump/IR probe study. *J. Am. Chem. Soc.* **2001**, *123*, 2255–2264.

(64) Snee, P. T.; Payne, C. K.; Mebane, S. D.; Kotz, K. T.; Harris, C. B. Dynamics of photosubstitution reactions of $\text{Fe}(\text{CO})_5$: An ultrafast infrared study of high spin reactivity. *J. Am. Chem. Soc.* **2001**, *123*, 6909–6915.

(65) Shelby, M. L.; Mara, M. W.; Chen, L. X. New insight into metalloporphyrin excited state structures and axial ligand binding from X-ray transient absorption spectroscopic studies. *Coord. Chem. Rev.* **2014**, *277*, 291–299.

(66) Shaik, S.; Chen, H.; Janardanan, D. Exchange-enhanced reactivity in bond activation by metal-oxo enzymes and synthetic reagents. *Nat. Chem.* **2011**, *3*, 19–27.

(67) Vanko, G.; Bordage, A.; Glatzel, P.; Gallo, E.; Rovezzi, M.; Gawelda, W.; Galler, A.; Bressler, C.; Doumy, G.; March, A. M.; Kanter, E. P.; Young, L.; Southworth, S. H.; Canton, S. E.; Uhlig, J.; Smolentsev, G.; Sundstrom, V.; Haldrup, K.; van Driel, T. B.; Nielsen, M. M.; Kjaer, K. S.; Lemke, H. T. Spin-state studies with XES and RIXS: From static to ultrafast. *J. Electron Spectrosc. Relat. Phenom.* **2013**, *188*, 166–171.

(68) Clark, J. N.; Beitra, L.; Xiong, G.; Higginbotham, A.; Fritz, D. M.; Lemke, H. T.; Zhu, D.; Chollet, M.; Williams, G. J.; Messerschmidt, M.; Abbey, B.; Harder, R. J.; Korsunsky, A. M.; Wark, J. S.; Robinson, I. K. Ultrafast three-dimensional imaging of lattice dynamics in individual gold nanocrystals. *Science* **2013**, *341*, 56–59.

(69) Dell'Angela, M.; Anniyev, T.; Beye, M.; Coffee, R.; Foehlich, A.; Gladh, J.; Katayama, T.; Kaya, S.; Krupin, O.; LaRue, J.; Mogelhoff, A.; Nordlund, D.; Norskov, J. K.; Oberg, H.; Ogasawara, H.; Ostrom, H.; Pettersson, L. G. M.; Schlotter, W. F.; Sellberg, J. A.; Sorgenfrei, F.; Turner, J. J.; Wolf, M.; Wurth, W.; Nilsson, A. Real-time observation of surface bond breaking with an X-ray laser. *Science* **2013**, *339*, 1302–1305.

(70) Kubacka, T.; Johnson, J. A.; Hoffmann, M. C.; Vicario, C.; de Jong, S.; Beaud, P.; Gruebel, S.; Huang, S. W.; Huber, L.; Patthey, L.; Chuang, Y. D.; Turner, J. J.; Dakovski, G. L.; Lee, W. S.; Minitti, M. P.; Schlotter, W.; Moore, R. G.; Hauri, C. P.; Koohpayeh, S. M.; Scagnoli, V.; Ingold, G.; Johnson, S. L.; Staub, U. Large-amplitude spin dynamics driven by a THz pulse in resonance with an electromagnon. *Science* **2014**, *343*, 1333–1336.

(71) Trigo, M.; Fuchs, M.; Chen, J.; Jiang, M. P.; Cammarata, M.; Fahy, S.; Fritz, D. M.; Gaffney, K.; Ghimire, S.; Higginbotham, A.; Johnson, S. L.; Kozina, M. E.; Larsson, J.; Lemke, H.; Lindenberg, A. M.; Ndabashimiye, G.; Quirin, F.; Sokolowski-Tinten, K.; Uher, C.; Wang, G.; Wark, J. S.; Zhu, D.; Reis, D. A. Fourier-transform inelastic X-ray scattering from time- and momentum-dependent phonon-phonon correlations. *Nat. Phys.* **2013**, *9*, 790–794.